International Journal of Industrial Electronics, Control and Optimization IECO
Vol. 5, No. 2, pp.167-176, April (2022)

An Electrical Energy Regeneration Scheme for Energy Harvesting From a Vibration Absorption System in Tall Buildings

Mohammad A. Beladi Pour[1], Amir H. Abolmasoumi[2†], Mehdi Soleymani[3] , Mazdak Ebadi[4]

[1] Department of Mechatronics, Arak University, Arak, Iran,
[2,4] 1. Electrical Engineering Department, Arak University, Arak, Iran, Research Institute of Renewable Energy, Arak University, Arak, Iran,
[3] Department of Mechanical Engineering, Arak University, Arak, Iran,

ABSTRACT

Electrical energy regeneration and storage in a tall structure with the installed passive pendulum tuned mass and damper (PPTMD) is investigated. While the passive vibration absorbing system works as an energy harvesting device, an electrical system including an electric motor, power electronic converters, a battery charger and storage subsystem are designed in order to store the energy taken from the structure vibrations which may be resulted from various external disturbances such as wind or earthquakes. The whole 76-story structure and the relevant electrical energy regeneration system are modeled and simulated and the design scheme is implemented on a two-story reduced order lab structure equipped with PPTMD, the electronic circuit and the battery. A boost AC rectifier is designed and controlled to rectify the AC output voltage and is followed by a boost DC-DC converter as a battery charger for the Li-ion battery. A passivity-based controller (PC) and a sliding mode controller are designed for the rectifier and the battery charger, respectively. The simulation and the real test results demonstrate the efficient harvesting and storage of the energy extracted from the building.

Article Info

Research Article

Keywords:

Boost AC rectifier, Boost DC-DC converter, Energy regeneration Passivity-based control, Passive tuned mass damper Sliding mode control.

Article History:

Received 2022-01-31
Accepted 2020-05-20

I. INTRODUCTION

Recent architecture of buildings in modern cities of high population has moved towards tall structures with some movement flexibility [1,2] where the external disturnbance loads such as wind and seismic forces are potential treats to the stability of such structures. The emerging of structural control systems is a response to the urgent need of building stabilization [3,4]. There are several types of such systems reported in the literature such as passive-type [3,5] , the semi-active-type [6,7] and active-type solutions [8-12]. As the most commonly used and easy to implement solutions, passive-type systems include the simple methods such as the base isolation solution [13] and viscoelastic dampers solutions [14], or different kinds of the the vibration absorbing systems such as tuned mass dampers (TMDs) [15], tuned liquid column dampers (TLCDs) [16], and pendulum-based TMDs (PTMDs) [17,18], etc. All mentioned types of passive vibration absorber systems have as their objective the damping of the structural vibrations resulted from the external disturbances.

The passive-type vibration absorbing systems used for the structural control consume less amount of energy as compared to other systems such as the semi-active and active ones since they need no source of power for their operation. However, the

†Corresponding Author: a-abolmasoumi@araku.ac.ir
Tel: +98-32625620,
1. Electrical Engineering Department, Arak University, Arak, Iran,
2. Research Institute of Renewable Energy, Arak University, Arak, , Iran

Copyright © 2022 Abolmasoumi et al. Published by University of Sistan and Baluchestan. This work is licensed under a Creative Commons Attribution-Noncommercial 4.0 International license. (https://creativecommons.org/licenses/by-nc/4.0/). Non-commercial uses of the work are permitted, provided the original work is properly cited

energy of the vibration that is absorbed by the passive-type device, for example an installed pendulum, is completely dissipated. To harvest such otherwise-wasted energy from the building vibrations an energy conversion unit together with an especial design is needed. The recovered energy can be later utilized as the common utility electric power or be stored in the building emergency power storage system. Extracting of energy from vibrating systems has been previously studied in [19-22]. There are few studies regarding the energy regeneration in the passive structural systems. For example, in [23] the extraction of energy from through-building openings openings is investigated. Authors in [24] sduggest the extraction of the energy from the engineered cementitious composites by using the polyvinylidene fluoride piezo polymer. In [25] energy harvesting from a TMD system is studied. Also in [26] authors design a pendulum-based energy regenerating systems to provide the energy for the wireless sensor network installed in the structure when under seismic forces.

As the power generated by pendulum-based compensators is of oscillatory nature, to store such power there is a need to convert the power to a DC output with minimum fluctuations. In this paper, an scheme for restoring the power from the pendulum actuator is proposed and the electronic processing and control of such power to be finally stored in the battery system. To this aim a DC generator followed by an AC rectifier system is utilized in order to simultaneously rectify and convert the semi-AC voltage into amplified DC voltage prior to being boosted through the DC-DC converter. The AC rectifier unit includes a passivity-based PWM control (PC) which adjusts the output DC voltage. Afterwards, a boost DC-DC converter is responsible to enhance and tune the voltage and also acts as the battery charger system to adjust the fixed charging current according to the charging plan of the Li-ion battery. A sliding mode controller has been designed using the augmented nonlinear dynamic model of the battery to fix the battery charging current. There several application of sliding mode controllers on DC-DC converters (See for example [27-28] and the references therein). Here, a simple sliding mode controllers is designed based on the augmented dynamic model of the battery/converter to adjust the battery charging current.

The whole two-story structure and energy regeneration generator has been experimentally constructed and installed over a shake table. To have a better visibility of results the electronic processing and storage system including converters and batteries are simulated in Matlab Simulink and linked to the hardware to form a harware-in-loop test setup. The results show the effective implementation of the proposed scheme in regenerating the power from the PTMD actuator.

The novelty of this paper is threefold: (1) this paper presents a complete scheme for energy regeneration from PPTMD. The plan is a multi-stage energy regeneration scheme that has not been previously proposed. (2) A passivity-based control design for the AC rectifier system has been designed (3) a sliding mode controller has been designed for the boost DC-DC

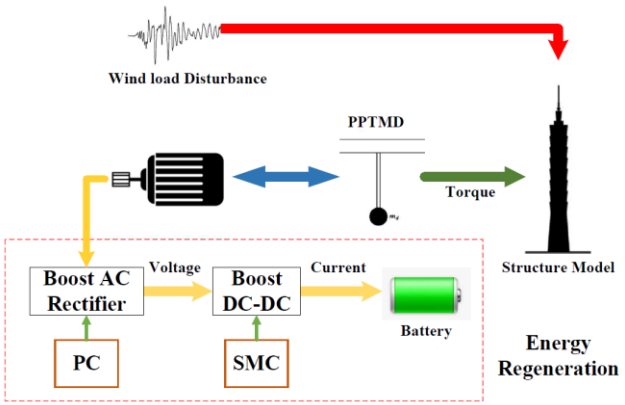


Fig. 1. The overall plan of energy regeneration from passively damped structure including PPTMD.

battery charger using the unified model of the converter/battery.

The rest of the paper is organized as follows: Section II firstly gives the basics on energy regeneration from a passively damped structure and then each component of the energy regeneration system is introduced in detail. The designed dynamic controllers are also discussed. Section IV represents the simulation and test results regarding the implementation of the regeneration system. Finallly, section V concludes the paper.

II. Energy Regeneration Scheme

The vibrations from different external forces such as wind and earthquake are devastating factors considered in the design and operation of tall buildings. Tuned mass-damper (TMD) systems are common devices which are employed to absorb the kinetic energy of the structure vibrations. In this study, a structure with an installed passive-pendulum-type TMD (PPTMD) is considered. The pendulum is usually installed on the upper floors where the most intense movements occur [17, 18]. In our energy regeneration scheme, an electric motor is coupled along the pendulum joint to transform the mechanical energy of the pendulum swings to the electrical energy. The outcome electric voltage is then rectified and converted to DC voltage. The electrical energy is finally stored in a Li-ion battery via a charger circuit. The described structure including the PPTMD, the electric motor and the power electronic circuit is shown in Figure 1.

The dynamic equations of the structure movements are described as ([29])

$$\mathbf{M}\ddot{\boldsymbol{x}}+\mathbf{C}\dot{\boldsymbol{x}}+\mathbf{K}\boldsymbol{x}=\left(-\mathbf{M}\{\mathbf{r}\}\{\ddot{u}_g\}\boldsymbol{or}\{\mathbf{E}\}\{f_w(t)\}\right) \quad (1)$$

in which $\boldsymbol{x}$ is the vector of the displacements. The centered masses of floors are represented as the following diagonal

matrix

$$\mathbf{M} = \begin{pmatrix} m_1 & \dots & 0 \\ \vdots & \ddots & \vdots \\ 0 & \dots & m_n \end{pmatrix} \quad (2)$$

and the stiffness matrix **K** is represented as

$$\mathbf{K} = \begin{pmatrix} k_1 + k_2 & 0 & 0 & \dots & 0 \\ -k_2 & \ddots & 0 & 0 & \vdots \\ \vdots & 0 & k_{ij} & 0 & 0 \\ 0 & 0 & 0 & \ddots & -k_n \\ 0 & \dots & 0 & 0 & k_n \end{pmatrix} \quad (3)$$

where k_i is the stiffness of the *i*-th floor. The damping matrix *C* in (1) is described as

$$\mathbf{C} = a_0\mathbf{M} + a_1 \quad (4)$$

where a_0 and a_1 are calculated in terms of stiffness of floors and the natural frequencies of the structure as

$$a_0 = \frac{2\xi w_1 w_3}{w_1 + w_3},\ a_1 = \frac{2\xi}{w_1 + w_3}$$

where w_1, w_2, w_3 are first three structural modes [29]. In (1), $\ddot{u}_g$ is the external disturbance acceleration and **r (**or **E)** is the disturbance excitation coefficient matrix and $f_w(t)$ is the wind force. The dynamic equation describing the pendulum swing is expressed as

$$\ddot{\theta} = -\left(\frac{g}{L_p}\right)\sin\theta - \frac{\ddot{x}_h}{ML_p^2} + \left(\frac{1}{ML_p^2}\right)T \quad (5)$$

where x_h is the top story displacement, g represents the gravity acceleration, L_p is the pendulum arm length, T is the outcome torque and θ is the swing angle. In case the pendulum axis is coupled with a generator shaft, the mechanical torque T contributes to the electrical energy production by the pendulum system which should be later processed to be stored in the battery. The length and mass of the pendulum is determined according to the natural frequency of the structure and its first modal mass [30]. Such energy is not currently harvested in the passively damped structures. In order to harvest and store such energy a generator system together with power electronic devices are employed. The complete diagram of energy regeneration has been depicted in Figure 1. As seen, the pendulum joint is coupled with a DC generator to transform the output mechanical power into an almost-AC electric power. The output voltage of the generator is rectified and regulated using an AC rectifier. The result is a DC voltage of desired magnitude. The output is then applied to a DC-DC boost converter that acts as a current charge controller for the battery. The resulting power is restored in Li-ion battery. In the following, different parts of the energy regeneration system together with the relevant control strategies are explained.

TABLE I
SPECIFICATIONS OF THE DC GENERATOR

Parameter	Unit	Simulated 76-story building	Two-story structure
Maximum Power	W	4500	12
Nominal Voltage	V	400	12
Nominal Current	Amp	10	1
Electric inductance (L)	μH	100.5	10
Electric resistance (Ra)	Ohm	3.5	1.1
Friction coefficient (B)	N.m.s	0.002	0.001
Moment of inertia (J)	Kg/m^2	0.001	0.01
Torque constant (K)	N.m/Amp	1.8	0.2

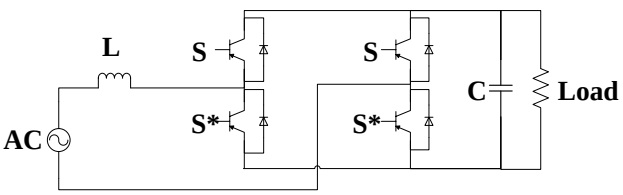


Fig. 2. Structure of the AC rectifier.

A. Electric DC Generator

The electric DC generator is coupled with the pendulum installed on the upper floor of the structure. The motor include a gearbox system to adjust the rotational speed and torque and is connected to the pendulum joint on the structure. The DC generator is of the permanent-magnet type. The specifications of the used DC electric motor for a 76-story and the one used for the reduced-order two-story lab structure in this study, are given in Table I.

B. AC Rectifier

The output voltage of the DC generator is almost AC while including contaminations of higher frequencies. It means that the voltage is of alternative nature as a result of the swing movements of the pendulum; however, it may include harmonics of different orders. In order to store the electric voltage extracted from the structural movements it is necessary to convert it into the DC voltage. Moreover, the magnitude of such voltage is usually low. It is because the output voltage depends on the rotational speed/frequency of the swing and such rotational speed is usually low. Such voltage will then undergo some processing by the power electronic circuits to be finally stored in the batteries. As each circuit causes some voltage loss, it is essential for the voltage magnitudes to be high enough before applying to the battery charger. Employing a gearbox system can slightly improve the voltage magnitude, however, it is still needed to provide a higher voltage. To obtain the regulated DC voltage from the input AC-like

voltage, using the conventional bridge rectifiers is not recommended. Instead, a boost AC rectifier can be used here that converts the voltage into DC and amplifies the magnitude at the same time. Boost rectifier or boost AC rectifier is a well-known interface circuit in power electronics. In some references it is also called the power factor correction (PFC) boost rectifier. Such circuit increases the power factor and reduces harmonic currents. As a result, the circuit is usually used for improving the power quality of power supplies. For general description on these circuits please refer to [31-34]. Here, the boost AC-DC circuit is used to convert the DC voltage to AC voltage and, in the same time amplify the magnitude of voltage. The circuit diagram of the used AC rectifier is depicted in Figure 2. The circuit includes four switches, a capacitor, and an inductor connected to the resistance load.

The dynamic equations of the single phase boost AC rectifier is given as follows ([35]):

$$\begin{aligned} L\frac{di}{dt} &= -uV + \bar{V}_{AC}, \\ C\frac{dV}{dt} &= ui - \frac{1}{R}V, \end{aligned} \tag{6}$$

where $\bar{V}_{AC} = E\sin(\omega_0\tau)$, is the ideal input AC voltage, i is the input current, V is the output DC voltage, u is the average duty-cycle of the PWM input applied to the switch gates, L is the inductance, R is the resistance, C is the capacitance and E is the AC voltage magnitude. Using the time-scale change $\tau = t/\sqrt{LC}$ defining the quality factor $Q = R\sqrt{C/L}$, and the normalized states $x_1 = (i/E)\sqrt{L/C}$, $x_2 = V/E$, the average state-space equations of the boost AC rectifier could be rewritten as follows:

$$\begin{cases} \dot{x}_1 = -ux_2 + V_{AC}, \\ \dot{x}_2 = ux_1 - \dfrac{x_2}{Q}, \end{cases} \tag{7}$$

where $V_{AC} = \sin(\omega_0\tau)$ could be the ideal normalized input. Here a passivity-based controller is designed to adjust the level of the output voltage. It is assumed that the desired state trajectory $x^*(\tau)$ also satisfies

$$\begin{aligned} \dot{x}_1^* &= -u^* x_1^* + V_{AC}, \\ \dot{x}_2^* &= u^* x_1^* - \frac{x_2^*}{Q}, \end{aligned} \tag{8}$$

By defining the state tracking error $e = x(\tau) - x^*(\tau)$ it can be easily shown that the error dynamics are obtained as

$$\begin{aligned} \dot{e}_1 &= -ue_2 - x_2^* e_u, \\ \dot{e}_2 &= ue_1 - \frac{e_2}{Q} + x_1^* e_u, \end{aligned} \tag{9}$$

where $e_u = u - u^*$. Now suppose that the control is designed such that $e_u = -\gamma\left(-x_2^* e_1 + x_1^* e_2\right)$ for some positive γ. Replacing to (9) results in

$$\begin{aligned} \dot{e}_1 &= -ue_2 + \gamma x_2^*\left(-x_2^* e_1 + x_1^* e_2\right), \\ \dot{e}_2 &= ue_1 - \frac{e_2}{Q} - \gamma x_1^*\left(-x_2^* e_1 + x_1^* e_2\right), \end{aligned} \tag{10}$$

Defining the error energy as $V = 0.5(e_1^2 + e_2^2)$ leads to

$$\begin{aligned} \dot{V} &= e_1\left[-ue_2 - \gamma(x_2^*)^2 e_1 + \gamma x_1^* x_2^* e_2\right] \\ &\quad + e_2\left[ue_1 - \frac{e_2}{Q} + \gamma x_1^* x_2^* e_1 - \gamma(x_1^*)^2 e_2\right] \\ &= -\gamma(x_2^*)^2 e_1^2 + 2\gamma x_1^* x_2^* e_1 e_2 - \gamma(x_1^*)^2 e_2^2 - \frac{e_2^2}{Q}. \end{aligned} \tag{11}$$

In order to have negative value for the Lyapunov time derivative the following inequality, referred to as dissipation matching condition, should hold:

$$\begin{bmatrix} \gamma(x_2^*)^2 & \gamma x_1^* x_2^* \\ \gamma x_1^* x_2^* & -\dfrac{1}{Q} - \gamma(x_1^*)^2 \end{bmatrix} > 0 \tag{12}$$

The controller is then calculated as

$$\begin{aligned} u &= u^* + \gamma\left[x_2^*\left(x_1 - x_1^*\right) - x_1^*\left(x_2 - x_2^*\right)\right] \\ &= u^* + \gamma\left(x_2^* x_1 - x_1^* x_2\right) \end{aligned} \tag{13}$$

It is needed to choose the desired state trajectory values x_1^* and x_2^* in calculation of control. If the total average energy of the system is $E = 0.5(x_1^2 + x_2^2)$ then the power is given by

$$\frac{dE}{dt} = x_1 V_{AC} - \frac{x_2^2}{Q}, \tag{14}$$

in which the first term is the input power and the second is the delivered power. In the balance condition the dc values of two terms are equal that gives

$$\left\langle \bar{x}_1 V_{AC} \right\rangle_{dc} = \left\langle \frac{\bar{x}_2^2}{Q} \right\rangle_{dc}. \tag{15}$$

The desired state trajectory values can be selected by considering (15). In an ideal case, the normalized output voltage x_2 converge to the steady state dc value V_d and the normalized AC current have the steady state $\bar{x}_1 = A\sin(\omega_0\tau)$. Setting also $V_{AC} = \sin(\omega_0\tau)$ we have

$$A = \frac{2V_d^2}{Q}, \tag{16}$$

Therefore, the steady state values $x_2^* = V_d$, $x_1^* = A\sin(\omega_0\tau)$ are appropriate choices. In (13) it is also needed to calculate u^* that can be obtained from (8) as

$$u^* = \frac{V_{AC} - \dot{x}_1^*}{x_2^*} \tag{17}$$

which in case of ideal AC input becomes

$$u^* = \frac{\sin(\omega_0\tau) - A\omega_0\cos(\omega_0\tau)}{V_d}. \quad (18)$$

Thus, as a summary, the PC can be designed as

$$u = u^*(\tau) + \gamma\left[x_2^* x_1 - x_1^* x_2\right],$$
$$u^* = \frac{\sin(\omega_0\tau) - A\omega_0\cos(\omega_0\tau)}{x_2^*}, \quad (19)$$
$$x_1^* = A\sin(\omega_0\tau),\ x_2^* = V_d,\ A = 2V_d^2/Q.$$

where V_d is the desired DC voltage ratio and γ is a positive design parameter to adjust the speed and damping of the transient response.

C. Battery Charging Circuit

The boost AC rectifier provides the regulated DC voltage with the desired magnitude. Such voltage level is determined by the battery specifications. However, the rectifier is not able to control the input current for charging the battery. Consequently, a charge controller circuit is needed to control the charging current. To this aim, a boost DC-DC converter is suggested as the battery charger. The application of DC-DC converter as the battery charger is studied by several researchers (see for example [36, 37] and the references therein). The circuit diagram of the boost DC-DC converter is shown in Figure 3. The output current of the boost DC-DC converter should be controlled for the goal of ensuring the efficient battery charge-time and its long-time health. The dynamic state-space equations of the boost DC-DC converter is described as follows:

$$L\frac{di}{dt} = -(1-u)V + V_{in},$$
$$C\frac{dV}{dt} = (1-u)i - i_{bat},$$
$$\frac{dSOC}{dt} = i_{bat},$$
$$i_{bat} = \frac{V - E_{oc}}{R_0}, E_{oc} \approx \alpha SOC + \beta, \quad (20)$$

where i is the input current, V is the output DC voltage, i_{bat} is the battery input current, $u \in [0,1]$ is the on-off input applied to the switch gate, SOC is the state of charge of the battery, E_{oc} is the open-circuit voltage of the battery, L is the inductance, R_0 is the battery internal resistance, and V_{in} is the input voltage. Also, parameters α, β are describing the dependency of the open-circuit voltage of the battery on its charging level. Here, this relationship is approximately assumed to be linear.

To regulate the charging current a sliding mode controller is designed using the unified dynamic model of the boost DC-DC and the battery. The sliding surface is defined as $S = i_{bat} - \bar{i}_{bat}$ in which $\bar{i}_{bat}$ is the desired charging current. The equivalent control u_{eq} is obtained by setting $\dot{S} = 0$. According to (20), this results in

TABLE II
SPECIFICATIONS OF THE BATTERY AND ELECTRONIC CIRCUITS

Device	Parameter	76-story structure	Two-story structure
Battery Cell	Rated capacity (Ah)	4500	0.018
	Internal resistance (Ohm)	400	1.777
	Nominal voltage (V)	10	3.2
AC Rectifier	Inductance (mH)	2	0.5
	Capacitance (μF)	1000	10
Boost DC-DC	Inductance (mH)	1	0.1
	Capacitance (μF)	4700	1000

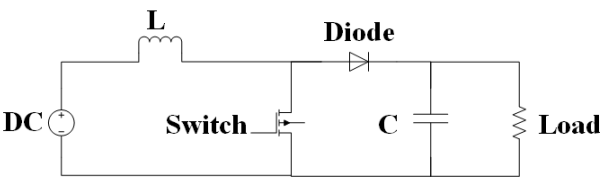


Fig. 3. Structure of the battery charging system.

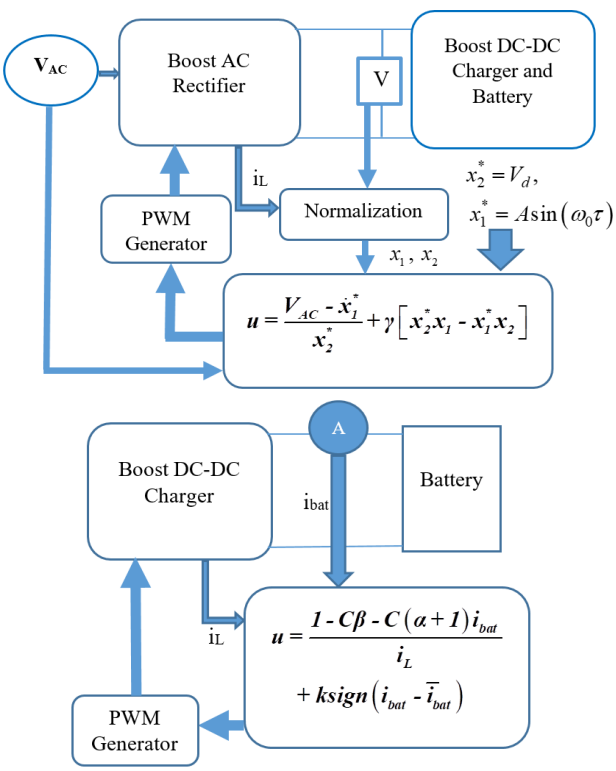


Fig. 4. A block diagram of control system.

$$u_{eq} = \frac{1 - C\beta - C(\alpha+1)i_{bat}}{i}. \quad (21)$$

The whole sliding mode control is then expressed as

$$u = u_{eq} + ksign(S) \quad (22)$$

The sliding gain k can be then chosen large enough to guarantee the stability of the sliding surface.

The specification of the required battery, and the component values of the boost AC rectifier and the boost DC-DC converter is given in Table II. The size of the battery-pack is determined using a serial-parallel cell arrangement. The implementation of the control methods are also shown in Figure 4.

III. Simulations and Test Results

To evaluate the implementation of the proposed energy regeneration scheme, the overall plan is simulated on two-story and 76-story buildings. Moreover, laboratory test results are taken from a two-story experimental lab structure that is constructed based on the reduced model of an eleven-story building. Since the level of the generated voltage at the terminal of the DC generator installed on the laboratory structure is too low to be processed in actual electronic circuits, a hardware-in-loop test system was used to interface the laboratory structure, the pendulum and the corresponding coupled generator with the LabVIEW software in the PC where the electronic circuits are simulated.

A. Simulation Results

A two-story and a 76-story building with the regeneration system are simulated. It should be noted that the first goal of PPTMD system is to reduce the oscillations of the structure under the effect of the external disturbances such as earthquake or wind. Thus, firstly the performance of the passive pendulum in the structure stabilization is demonstrated.

For the two-story building only the earthquake force is considered to be effective while for the 76-story building the wind effect has been simulated. For the simulated two-story building the parameters are as follows:

$$M=\begin{pmatrix}3.7769 & 0\\ 0 & 3.2372\end{pmatrix}, K=\begin{pmatrix}511.4320 & -322.1163\\ -322.1163 & 322.1163\end{pmatrix},$$

$$C=\begin{pmatrix}3.3703 & -1.3951\\ -1.3951 & 2.3853\end{pmatrix} \quad (23)$$

A pendulum with the length equal to 60 cm and the mass equal to 500g is used. To induce the structural movements, the data from *El Centro* earthquake has been utilized [38] whose acceleration profile is given in Figure 5. Also Figure 6 shows the time variations of the upper floor's displacement and velocity for the passively-damped structure compared to the undamped one. As seen, the passive pendulum system leads to a decrease in the structural movements. The effect of wind has been studied on a 76-story building. The wind force is calculated as

$$F=\frac{1}{2}\rho A_z^2 C_d V_{z,t}^2 \quad (24)$$

where $V_{z,t}$ is the wind speed, C_d is the aerodynamic drag coefficient, A_z is the effective area and ρ is the air density.

For 76-sotry building, a PPTMD system with the mass of 1000kg and the length of 2.5m is considered that is installed

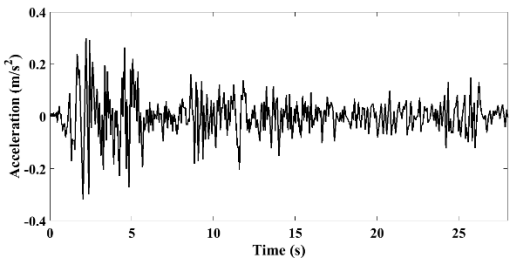
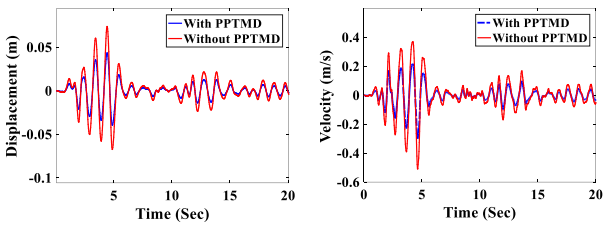
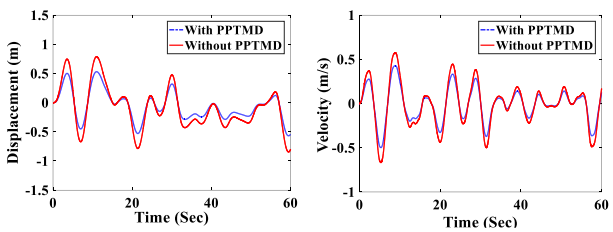


Fig. 5. El Centro earthquake acceleration profile used as the structure disturbance force [38].



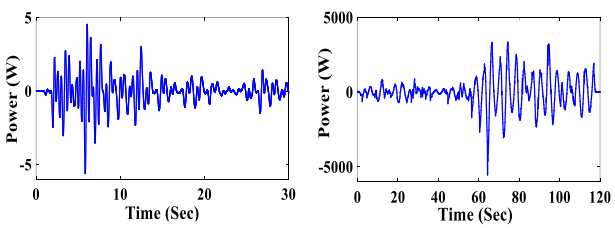
(a) (b)

Fig. 6. Upper floor's movements for the simulated two-story building (a) displacement (b) velocity.



(a) (b)

Fig. 7. Top floor's movements for the simulated 76-story building (a) displacement (b) velocity.



(a) (b)

Fig. 8. The active power damped by the PPTMD without energy regeneration for (a) simulated two-story building under earthquake (b) 76-story building under wind force.

on the upper floor. Figure 7 shows the top floor's displacement and velocity with and without PPTMD system which clearly shows the superiority of the PPTMD system in stabilizing the structural movements. The active powers damped by the PPTMD for both simulated structures are depicted in Figure 8. Such power may be utilized by conversion into the electrical power, processing and finally storing in the batteries. For the

76-story, however, the actual wind calculations are used.

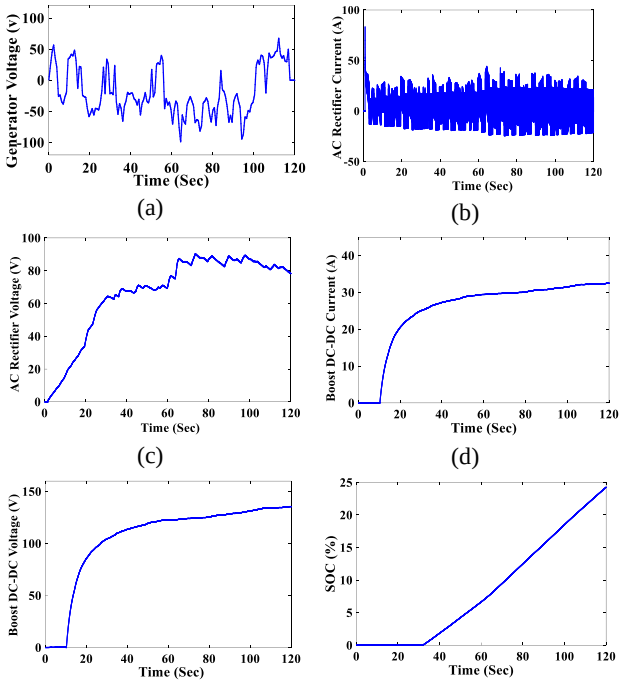


Fig. 9. Electrical signals at different stages of the power processing for the simulated 76-story building: (a) output voltage of the pendulum-coupled generator (b) input current of boost AC rectifier (c) output voltage of boost AC rectifier (d) input current to boost DC-DC converter (battery charger) (e) battery charger voltage (f) state of charge of the battery.

The electric voltages and currents at different stages of the power processing are shown in Figure 9 that demonstrates the satisfactory performance of the proposed plan. Figure 9(a) represents the voltage produced by the generator as a result of the movements of the pendulum installed on a 76-story building. In this case the pendulum absorbs the movements of the structure by the wind. The current of the boost AC rectifier is shown in Figure 9(b). The reasons for high frequency of the current is the assumption that in PC the input voltage is ideally sinusoidal signal with fixed frequency while it is not true for the case of 76-story building. PC makes use of the derivative of the voltage that may results in high frequency control input and the possible high frequency current. The effect of the SMC control on the DC-DC charger may also induce high frequencies on the boost AC rectifier.

Figure 9(c) shows the almost DC voltage as the output of the boost AC rectifier. The non-smooth DC voltage is again due to the non-sinusoidal voltage of the generator. However, this is fixed by the boost DC-DC charger as the current and voltage are almost DC (Figures 9(c) and 9(d)) and the state-of-charge is increasing with time with fixed current (Figure 9(f)).

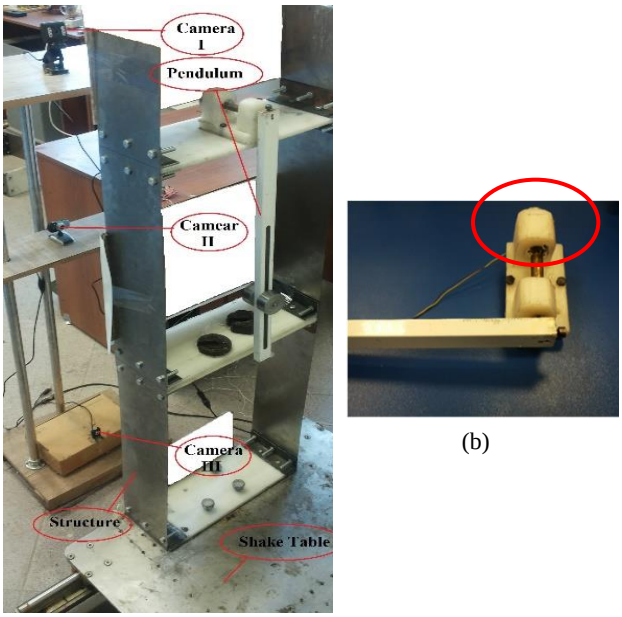


Fig. 10. The laboratory setup of the regenerative PPTMD: (a) The whole structure (b) the pendulum and the coupled generator.

B. Experimental Results

In addition to simulation of the proposed plan by using the modeling principles, the proposed energy regeneration scheme is implemented on a laboratory structure. The two-story structure, i.e. the reduced model of an 11-story building by mimicking its major natural frequencies, is installed on a single-axis laboratory shake table. The shake table is controlled using the LabVIEW software on the PC exchanging the data with an AC servo drive via data acquisition cards. The servo drive controls the the shake table to generate any desired acceleration profile. Previous researches has been carried out the tracking control of the shake table taking into account various sensoring/control issues (See for example [38-41]). The laboratory setup is shown in Figure 10. Three PC-connected cameras are measuring the displacement and velocity of movements at different structure floors. The pendulum with appropriately calculated length, material and weight is installed on the top floor. The structure is composed of flexible metal sheets whose length, weight and elasticity are precisely calculated to reflect a real 11-story building in terms of the main natural frequencies. The details of the laboratory structure designed is available in [7, 9]. Figure 11 shows the results taken from the implemented setup in which the two-story structure, pendulum and the generator are real laboratory equipment and the electronic circuits and the battery are simulated in LabVIEW software and two parts of system are connected via a hardware-in-loop system. As seen in Figure 11, in this case, the voltage is rectified to a smooth DC voltage by the boost AC rectifier (see Figure 11(c))

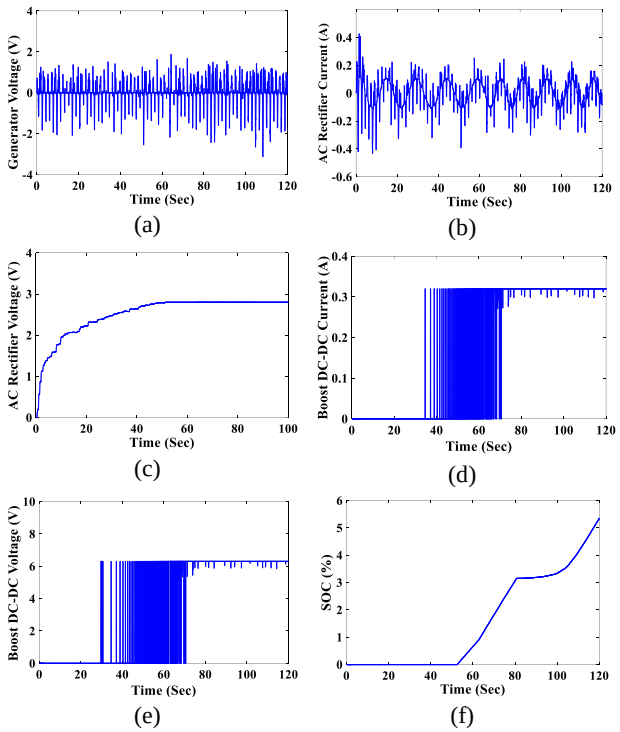


Fig. 11. Electric voltages at different stages of power processing for the laboratory test setup connected to the LabVIEW simulated electronic circuit and battery (a) output voltage of the pendulum-coupled (b) input current of boost AC rectifier (c) output voltage of boost AC rectifier (d) input current to boost DC-DC converter (battery charger (e) battery charger voltage (f) state of charge of the battery.

and the charging current is adjusted by the boost DC-DC charger (Figure 11(d)). The adjusted voltage and the increasing state-of-charge are also shown in Figures 11(e) and 11(f). The high frequency oscillations in the voltage and current is due to the intrinsic chattering caused by the SMC.

IV. Conclusions

An energy regeneration scheme for harvesting energy from a passive PTMD structural control system was proposed. The suggested plan includes a DC generator coupled with the damping pendulum. The output voltage produced by the electric motor was converted to a rectified DC by a boost AC rectifier that is controlled by a passivity-based control. A boost dc-dc converter is then utilized as the battery charger to guarantee the desired charging characteristics for the Li-ion battery. The boost charger is controlled by a sliding mode controller to address the nonlinear dynamics and model uncertainties of the converter and the battery. A 76-story building under wind force effect is simulated and the results show almost DC voltage as the output of the boost AC rectifier, DC output of the boost charger and the smooth charging current. Also the plan was experimentally implemented on a two-story laboratory structure mounted on a shake table. The electronic part was simulated within the PC using a hardware-in-loop system. The results from the experimental setup also verifies the efficiency of the proposed method in providing smooth DC output for the boost AC rectifier, and the desired charging characteristics for the battery charging system.

References

[1] M. M. Ali and K. S. Moon, "Structural developments in tall buildings: current trends and future prospects," *Architectural science review*, vol. 50, no. 3, pp. 205–223, 2007.

[2] Soong and B. Spencer Jr Reviewer, "Active structural control: theory and practice," *Journal of Engineering Mechanics*, vol. 118, no. 6, pp.1282–1285, 1992.

[3] B. Spencer Jr and S. Nagarajaiah, "State of the art of structural control," *Journal of structural engineering*, vol. 129, no. 7, pp. 845–856, 2003.

[4] B. Kavyashree, S. Patil, and V. S. Rao, "Review on vibration control in tall buildings: from the perspective of devices and applications," *International Journal of Dynamics and Control*, vol. 9, no. 3, pp.1316–1331, 2021.

[5] Parulekar and G. Reddy, "Passive response control systems for seismic response reduction: A state-of-the-art review," *International Journal of Structural Stability and Dynamics*, vol. 9, no. 01, pp. 151–177, 2009.

[6] M. D. Symans and M. C. Constantinou, "Semi-active control systems for seismic protection of structures: a state-of-the-art review," *Engineering structures*, vol. 21, no. 6, pp. 469–487, 1999.

[7] M. Soleymani, T. Asgari, and M. Sadeghi, "Design and implementation of a semi-active structural control system using shake table test," *Sharif Journal of Civil Engineering*, vol. 35, no.2.2, pp. 133–142, 2019.

[8] Korkmaz, "A review of active structural control: challenges for engineering informatics," *Computers & Structures*, vol. 89, no. 23-24,pp. 2113–2132, 2011.

[9] A. Khalatbarisoltani, M. Soleymani, and M. Khodadadi, "Online control of an active seismic system via reinforcement learning," *Structural Control and Health Monitoring*, vol. 26, no. 3, p. e2298, 2019.

[10] A. Preumont, Vibration control of active structures: an introduction. Springer, 2018, vol. 246.

[11] M. Soleymani, A. H. Abolmasoumi, H. Bahrami, A. Khalatbari-S, E. Khoshbin, and S. Sayahi, "Modified sliding mode control of aseismic active mass damper system considering model uncertainties and input time delay," *Journal of Vibration and Control*, vol. 24, no. 6,pp. 1051–1064, 2018.

[12] E. Khoshbin, A. H. Abolmasoumi, M. Soleymani, and A. Khalatbari, "Generalized active disturbance rejection control of structures under seismic disturbance considering time delays," *Structural Control and Health Monitoring*, vol. 25, no. 1, p. e2029, 2018.

[13] D. Botto and M. Umer, "A novel test rig to investigate under-platform damper dynamics," *Mechanical Systems and Signal Processing*, vol.100, pp. 344–359, 2018.

[14] S. Gong and Y. Zhou, "Experimental study and numerical simulationon a new type of viscoelastic damper with strong nonlinear characteristics," *Structural Control and Health*

Monitoring, vol. 24, no. 4, p.e1897, 2017.
[15] F. Rahimi, R. Aghayari, and B. Samali, "Application of tuned mass dampers for structural vibration control: a state-of-the-art review," *Civil Engineering Journal*, pp. 1622–1651, 2020.
[16] A. Di Matteo, T. Furtmuller, C. Adam, and A. Pirrotta, "Optimal design of tuned liquid column dampers for seismic response control of base-isolated structures," *Acta Mechanica*, vol. 229, no. 2, pp. 437–454, 2018.
[17] L. Wang, W. Shi, and Y. Zhou, "Study on self-adjustable variable pendulum tuned mass damper," *The Structural Design of Tall and Special Buildings*, vol. 28, no. 1, p. e1561, 2019.
[18] Wang, Liangkun, Weixing Shi, and Ying Zhou. "Study on self-adjustable variable pendulum tuned mass damper." *The Structural Design of Tall and Special Buildings*, vol. 28, no. 1, p e1561, 2019.
[19] H. S. Kim, J.-H. Kim, and J. Kim, "A review of piezoelectric energy harvesting based on vibration," *International journal of precision engineering and manufacturing*, vol. 12, no. 6, pp. 1129–1141, 2011.
[20] H. Wang, A. Jasim, and X. Chen, "Energy harvesting technologies in roadway and bridge for different applications–a comprehensive review," *Applied Energy*, vol. 212, pp. 1083–1094, 2018.
[21] H.-X. Zou, L.-C. Zhao, Q.-H. Gao, L. Zuo, F.-R. Liu, T. Tan, K.-X. Wei, and W.-M. Zhang, "Mechanical modulations for enhancing energy harvesting: Principles, methods and applications," *Applied Energy*, vol. 255, p. 113871, 2019.
[22] M. Gholikhani, H. Roshani, S. Dessouky, and A. Papagiannakis, "Acritical review of roadway energy harvesting technologies," *Applied Energy*, vol. 261, p. 114388, 2020.
[23] S. Hassanli, K. Chauhan, M. Zhao, and K. C. Kwok, "Application of through-building openings for wind energy harvesting in built environment," *Journal of Wind Engineering and Industrial Aerodynamics*, vol. 184, pp. 445–455, 2019.
[24] Y.-F. Su, R. R. Kotian, and N. Lu, "Energy harvesting potential of bendable concrete using polymer based piezoelectric generator," *Composites Part B: Engineering*, vol. 153, pp. 124–129, 2018.
[25] Y. Luo, H. Sun, X. Wang, L. Zuo, and N. Chen, "Wind induced vibration control and energy harvesting of electromagnetic resonant shunt tuned mass-damper-inerter for building structures," *Shock and Vibration*, vol. 2017, pp. 1-13. 2017.
[26] W. Shen, S. Zhu, H. Zhu, and Y.-l. Xu, "Electromagnetic energy harvesting from structural vibrations during earthquakes," *Smart structures and systems*, vol. 18, no. 3, pp. 449–470, 2016.
[27] G. Mohebalizadeh, H. Alipour, L. Mohammadian, and M. Sabahi, "An improved sliding mode controller for DC/DC boost converters used in EV battery chargers with robustness against the input voltage variations," International Journal of Industrial Electronics Control and Optimization, vol. 4, no. 2, p. 257-266, 2021.
[28] V. Utkin, "Sliding mode control of DC/DC converters," *Journal of the Franklin Institute*, vol. 350, no. 8, p. 2146-2165, 2013
[29] R. Clough and J. Penzien, "Dynamics of structures (3rd)," *Computers & Structures, Inc., California*, pp. 342–344, 2003.
[30] J. P. Den Hartog, *Mechanical vibrations*. Courier Corporation, 1985.
[31] D. Williams, "How the boost PFC converter circuit improves power quality," Available: https://www.allaboutcircuits.com/technical-articles/how-the-boost-pfc-converter-circuit-improves-power-quality/, 2016.
[32] J.C. Salmon, "Circuit topologies for single-phase voltage-doubler boost rectifiers," *IEEE Transactions on Power Electronics*, vol. 8, no. 4, p.521-529, 1993.
[33] J. Sastry, O. Ojo, and Z. Wu, "High-performance control of a boost AC–DC PWM rectifier/induction generator system," *IEEE transactions on industry applications*, vol. 42, no. 5, p.1146-1154, 2006.
[34] M. Monfard, M. Babaei, and S. Sharifi, "A z-source network integrated buck-boost PFC rectifier," International journal of industrial electronics control and optimization, vol. 2, no. 4, p.289-296, 2019.
[35] H. J. Sira-Ramirez, and S. O.Ramón, "Control design techniques in power electronics devices," Springer Science & Business Media, 2006.
[36] M. Feizi, R. Beiranvand, and M. Daneshfar, "An integrated high power self-equalized battery charger using a voltage multiplier and phase-shifted full-bridge DC-DC converter for lithium-ion batteries," International Journal of Industrial Electronics Control and Optimization, vol. 4, no. 2, p. 141-155, 2021.
[37] A. Taheri, and N. Asgari, "Sliding mode control of LLC resonant DC-DC converter for wide output voltage range in battery charging applications," International Journal of Industrial Electronics Control and Optimization, vol. 2, no. 2, p.127-136, 2019.
[38] P. Memarzadeh, M. Saadatpour, and M. Azhari, "Nonlinear dynamic response and ductility requirements of a typical steel plate shear wall subjected to El Centro earthquake," *Iranian Journal of Science and Technology Transaction B-Engineering*, vol. 34, no. B4, pp. 371-384, 2010.
[39] N. Rajabi, A. H. Abolmasoumi, and M. Soleymani, "Sliding mode trajectory tracking control of a ball-screw-driven shake table based on online state estimations using EKF/UKF," *Structural Control and Health Monitoring*, vol. 25, no. 4, p. e2133, 2018.
[40] M. Soleymani and A. H. Abolmasoumi, "Fuzzy-sliding mode supervisory control of an electric seismic shake table," *transformation*, p. 1, 2016.
[41] S. Sayahi, M. Hamidizadeh, H. Moradzadeh, M. Soleymani, and M. Rahmani, "Fuzzy control of a seismic shake table using a vision-based displacement measurement system." *Modares Mechanical Engineering*, vol. 14, no. 14, 2015.



Mohammad A. Beladi Pour was born in Gachsaran, Iran. He received his B.S. degree in Electrical Engineering majored in Control Engineering from Semnan University, Semnan, Iran in 2016 and his M.Sc. degree in Mechatronics from Arak University, Arak, Iran in 2018. From 2018 to 2019 he was collaboratingd with several knowledge-based enterprise companies. From 2020, he has worked as a researcher at Electronic Technology Institute, Shiraz, Iran. His Current research interests include nonlinear control, adaptive control, data driven methods, and machine vision systems.



Amir H. Abolmasoumi was born in Arak, Iran. He received his B.S. degree in control engineering from Tehran University, Tehran, Iran in 2005 and M.S. and Ph.D. degrees from Tarbiat Modares University, Tehran, Iran in 2008 and 2011, respectively. From then, he has been with the Electrical Engineering Department of Arak University, Arak, Iran. His main research interests include state estimation theory and applications in power and biological systems, Koopman operator theory, data-driven modeling, delay dynamic systems and structural control.



Mehdi Soleymani received his BSc, MSc, and PhD degrees from Iran University of Science and Technology (IUST) in 2000, 2003, and 2009 respectively. He was with Automotive Industry Research and Innovation Centre (AIRIC) of SAIPA Company as a senior test engineer from 2002 to 2004. He joined Arak University as an assistant professor of mechanical engineering and director of the system simulation and control laboratory in 2009. He has been with Arak University as an associate professor of mechanical engineering and mechatronics from 2015 up to the present. He joined Advanced Vehicle Engineering Centre (AVEC) of Cranfield University as a research fellow from 2018 to 2021. He is also an associate fellow of the higher education academy of UK. His research interest includes active vibration control of vehicular and structural systems, energy harvesting from vibration control systems in vehicles, tall buildings, and wind turbines, and design of control strategies and optimization algorithms for energy storage and energy management systems in hybrid electric, fuel cell, and electric vehicles.



Mazdak Ebadi was born in Booshehr, Iran. He received his B.S. degree in Electrical and Electronics Engineering from Shiraz University, Shiraz, Iran, in 2005, and his M.S. and Ph.D. degrees in Electrical Engineering from the Shahid Chamran University, Ahvaz, Iran, in 2008 and 2014, respectively. In 2014, he joined Arak University as an Assistant Professor in the School of Electrical and Electronics Engineering. His current research interests include Electrical Machinery, Power Inverters, DC-DC converters, and PWM converter/inverter systems.